Preprints of the 19th World Congress
The International Federation of Automatic Control
Cape Town, South Africa. August 24-29, 2014

Dual-mode Control Allocation for Integrated Chassis Stabilization

Rachid ATTIA, Rodolfo ORJUELA and Michel BASSET

Modélisation Intelligence Processus Systèmes (MIPS) laboratory, EA2332
Université de Haute-Alsace, 12 rue des Frères Lumière
F-68093 Mulhouse Cedex, France.
E-mail: firstname.lastname@uha.fr

Abstract: A hierarchical control architecture for lateral stabilization in automotive vehicles is proposed in this paper. The proposed direct yaw stabilization strategy is based on the optimal coordination of two conventional stabilization systems (differential brake and traction torque transfer). Thanks to this approach, high stabilization capabilities are obtained while the impact on the longitudinal motion is reduced. The control architecture is a three layer structure composed of a high-level control, an optimal control allocation and a low-level control. The main idea consists in the use of a dual-mode control allocation formulation to handle the different operating modes of the wheel according to available actuators, i.e. conventional braking and/or torque transfer. The performance of the integrated control strategy proposed is highlighted through simulation results.

1. INTRODUCTION

Considerable efforts have been devoted to the analysis of the lateral motion of the vehicle [Andreasson, 2007]. To enhance the vehicle handling in hard lateral manoeuvres several active safety systems such as ABS, AFS (Active Front Steering) and ESP (Electronic Stability Program) are developed. The ESP introduced by Bosch is based on a Direct Yaw Control (DYC) [Liebemann et al., 2004]. It is the widely used technique for lateral stabilization in the chassis control framework. The DYC consists in creating asymmetric longitudinal forces at the vehicle wheels in order to generate control moments around the vertical axis. The first generation of DYC are based on differential braking. The use of brake showed interesting capabilities even in hard lateral manoeuvres. However, the use of brakes largely affects the longitudinal dynamics of the vehicle. To cope with these drawbacks it is possible to use torque transfer to generate direct yaw moments [He et al., 2006]. Indeed, traction torque can be asymmetrically distributed between the traction wheels and this leads to asymmetric longitudinal forces generating a corrective yaw moment. This strategy affects fairly the longitudinal dynamics of the vehicle but its stabilizing abilities are limited compared to the brake based DYC [He et al., 2006]. In fact, the torque transfer for stabilization is appropriate in not extremal stabilizing situations as shown in [Hancock et al., 2005]. In this paper, both stabilizing techniques (brake and torque transfer) are implemented in an integrated stabilizing strategy to capitalize their advantages.

The objective of the combined control is to use the different systems in a synergy following an optimal design. Two approaches are commonly adopted to cope with the combined control problem [Hwang et al., 2008]. The first one is called the *unified approach*, in this approach the global control problem is handled by a single controller designed using multivariable system theory. However, the unified control design may be difficult due the system complexity induced by the subsystem interactions. The second one is called the *integrated approach*. In this one, several controllers dedicated to a given objective are integrated in a cooperative control architecture. The advantage of the integrated approach lays in the relative simplicity to design individually a controller for each objective. However, the integration of these controllers to perform global control objectives remains a challenge. From a technological point of view, the integrated approach corresponds to a distributed material architecture and this aspect is preferred by automotive manufacturers [Shibahata, 2005]. The problem of combining in an optimal way the torque transfer DYC and the brake DYC is considered here through a hierarchical control architecture.

The suggested architecture has three main control levels. The high-level controller determines a global moment, called also *generalized* or *virtual moment*, to ensure the vehicle lateral stability. The virtual moment is employed by the low-level control to calculate the real-world inputs of the available vehicle actuators (brakes, etc.). This task is carried out through an optimal distribution of the virtual moment among the actuator set using an Optimal Control Allocation (OCA) technique. Control allocation techniques are particularly adapted to cope with over-actuated systems, such as aircraft, automotive vehicle and ships,etc. For this kind of systems, the same control objective can be obtained by several combinations of the actuator effects (see [Johansen and Fossen, 2013] for a survey). Here, the authors propose a hierarchical control architecture and an Optimal Control Allocation to cope with this problem, a similar approach could be found in [Alberding et al., 2009]. The main contribution of the present paper lies in the use of a *dual-mode control allocation* formulation [Chen and Wang, 2012] to combine two conventional stabilization techniques in an integrated stabilization strategy. In fact, the dual-mode formulation helps to describe the two operating modes of the wheel corresponding to brake, torque transfer or combined brake/torque transfer.

The remainder of the paper is organized as follows. Section 2 is devoted to the lateral vehicle dynamics modelling. In Section 3 the hierarchical control architecture proposed in this

⋆ This work was supported by the Région-Alsace.

Copyright © 2014 IFAC

paper is presented. The conventional brake and torque transfer for lateral stabilization are briefly presented and compared in Section 4. Section 5 presents the main contribution results of this work. The integrated chassis stabilization through a dual-mode control allocation is described. Simulation results highlight the performance of the proposed approach compared to the conventional approaches.

2. VEHICLE MODELLING

This section is devoted to the description of the main dynamics governing the lateral motion of the vehicle. The lateral stability of the vehicle is directly related to the yaw and sideslip motions. The main external forces affecting the lateral dynamics are the longitudinal and lateral tire forces. The tire forces result from the tire-road contact due to the steering action as well as the brake and traction torques applied on each wheel.

2.1 Lateral Vehicle Dynamics Modelling

Fig. 1 shows a two-degrees-of-freedom (2DoF)-model of the vehicle motion with the main forces acting on the vehicle. For a constant speed and small sideslip angles, the lateral motion described by the sideslip angle β and yaw rate $\dot{\psi}$ dynamics is given by the following equations [Kiencke and Nielsen, 2000]:

$$mV\dot{\beta} = -mV\dot{\psi} + (F_{y_1} + F_{y_2} + F_{y_3} + F_{y_4}) \quad (1a)$$

$$I_z\ddot{\psi} = a(F_{y_1} + F_{y_2}) - b(F_{y_3} + F_{y_4}) + c(-F_{x_1} + F_{x_2} - F_{x_3} + F_{x_4}) \quad (1b)$$

where m and I_z respectively are the vehicle mass and the moment of inertia, V the vehicle speed, a and b the front and rear centre of gravity (CoG)-distances, c the track-width, F_{x_i} and F_{y_i} the longitudinal and lateral forces. The subscripts $\{i = 1,...,4\}$ refer respectively to the $\{front, left\}$, $\{front, right\}$, $\{rear, left\}$ and $\{rear, right\}$ wheels.

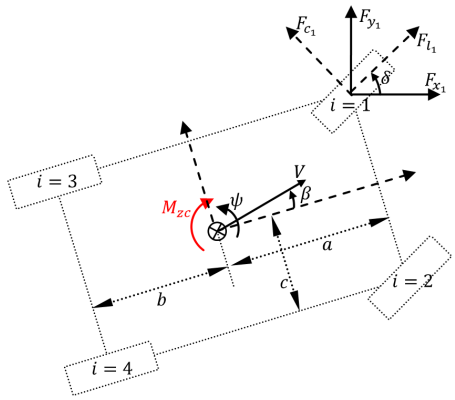

Fig. 1. 2DoF model of the vehicle

The forces F_{x_i} and F_{y_i} acting on the CoG of the vehicle are related to the tyre forces and the front steering angle δ as follows:

$$F_{x_{i=1,2}} = F_{l_{i=1,2}}\cos\delta - F_{c_{i=1,2}}\sin\delta, \quad F_{x_{i=3,4}} = F_{l_{i=3,4}} \quad (2a)$$

$$F_{y_{i=1,2}} = F_{l_{i=1,2}}\sin\delta + F_{c_{i=1,2}}\cos\delta, \quad F_{y_{i=3,4}} = F_{c_{i=3,4}} \quad (2b)$$

where the F_l and F_c are respectively the longitudinal and lateral tire forces. The longitudinal and lateral forces are function of the sideslip angle and the longitudinal motion following a nonlinear model of the form:

$$F_l = \mu_l(\lambda, \alpha, \mu)F_z \quad (3)$$

$$F_c = \mu_c(\lambda, \alpha, \mu)F_z \quad (4)$$

where F_z is the tire normal load, μ the road adhesion coefficient, α the wheel sideslip angle and λ the longitudinal slip ratio given by:

$$\lambda = \frac{V - R\omega}{\max(V, R\omega)} \quad (5)$$

where R is the wheel radius and ω the wheel rotational speed given by the wheel dynamics:

$$I_w\dot{\omega} = -F_lR + T_t - T_b \quad (6)$$

where T_t is the traction torque, T_b the braking torque and I_w the wheel moment of inertia. The longitudinal and lateral tire forces are related through the friction circle relationship expressed by:

$$\sqrt{F_l^2 + F_c^2} \leq \mu F_z \quad (7)$$

Here, it is assumed that each wheel can be individually braked and the vehicle is equipped with torque differential that allows torque transfer on the same axle. The road adhesion coefficient μ is assumed known.

2.2 Vehicle Lateral Handling Evaluation

Handling tests should be performed to show the effectiveness of the lateral stabilizing controllers. In [Forkenbrock et al., 2005] a set of different handling test manoeuvres used by the NHTSA to evaluate ESP effectiveness are presented. Among these test manoeuvres, the d-well sine manoeuvre is retained here. It is based on a single sinusoidal steering input shown in Fig. 2

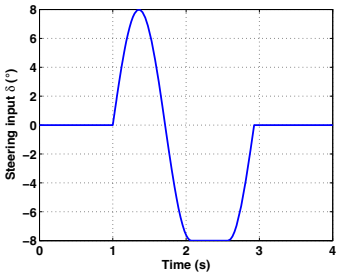

Fig. 2. Sine with Dwell Steering Input

A nonlinear 2DoF model with nonlinear Burckhardt's tire forces is used to evaluate the vehicle behaviour. This validation model takes also account of the lateral and longitudinal nonlinear couplings as well as the tire forces saturation. The manoeuvre is performed on a wet test-track ($\mu = 0.4$) at different entry speeds.

3. HIERARCHICAL CONTROL ARCHITECTURE FOR LATERAL STABILIZATION

The motion in the lateral direction is mainly governed by the total lateral forces. The yaw motion results of the combined lateral and longitudinal forces. The lateral forces are mainly induced by the driver's steering action. On the other hand, the longitudinal forces result of the slip motion at the tire-road interaction caused by brake and traction torques. The stabilization

system of interest here is based on a direct yaw control generated by differential longitudinal forces. The controller only uses brakes and torque transfer to provide the corrective yaw moment M_{zc}, non active steering is employed.

The corrective yaw moment M_{zc} could be generated using different combinations of the tire forces. The multiple manners allowing to achieve the same global objective, i.e. lateral stabilization, lead to an over-actuated system control problem. The Optimal Control Allocation (OCA) is a suitable technique to tackle this problem [Härkegard and Glad, 2005]. A high-level controller calculates the global action to be applied, here M_{zc}, to meet the control objectives. Then, the global action is distributed on the set of actuators following an OCA formulation. The proposed control architecture is summarized in Fig. 3.

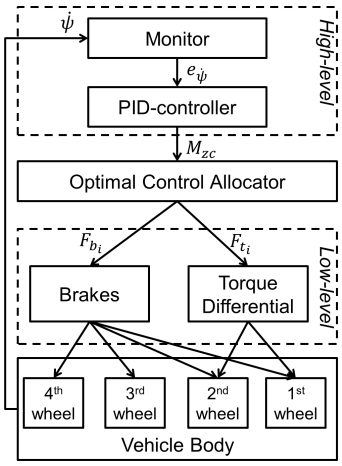

Fig. 3. Hierarchical control architecture

3.1 High-level Controller

The desired yaw rate $\dot{\psi}_{des}$ is determined here considering a 2DoF bicycle model with linear tire forces [Yoon et al., 2010]:

$$\begin{bmatrix}\dot{\beta}\\ \ddot{\psi}\end{bmatrix} = \begin{bmatrix}\frac{-2(C_f+C_r)}{mV} & \frac{2(-aC_f+bC_r)}{mV^2}-1\\ \frac{2(-aC_f+bC_r)}{I_z} & \frac{-2(a^2C_f+b^2C_r)}{I_zV}\end{bmatrix}\begin{bmatrix}\beta\\ \dot{\psi}\end{bmatrix} + \begin{bmatrix}\frac{2C_f}{mV}\\ \frac{2aC_f}{I_z}\end{bmatrix}\delta \quad (8)$$

where C_f and C_r are respectively the stiffness coefficients of the front and rear tires, such that:

$$F_{c_{i=1,2}} = -C_f\alpha_f \quad \text{and} \quad F_{c_{i=3,4}} = -C_r\alpha_r \quad (9)$$

with α_f and α_r the front and rear wheel sideslip angles.

At the steady-state yaw rate ($\ddot{\psi}=0$), the vehicle manoeuvre is supposed to reflect the driver's intention and the corresponding yaw rate is expressed as a function of the vehicle speed V and the steering input δ, as follows:

$$\dot{\psi}_{des} = \frac{2C_fC_r(a+b)^2}{2C_fC_r(a+b)^2 - (m(aC_f-bC_r)V^2)}\frac{V}{a+b}\delta \quad (10)$$

The yaw rate tracking error is then given by:

$$e_{\dot{\psi}} = \dot{\psi} - \dot{\psi}_{des} \quad (11)$$

The high-level controller is also composed of a monitoring policy determining the activation of the stabilization control. The stabilizing controller is activated when a critical situation is detected based on lateral stability criteria available in the literature [Tondel and Johansen, 2005]. When the stabilizing controller is active, it calculates the corrective yaw moment M_{zc} that ensures the lateral stability of the vehicle. Here, the stabilizing controller is based on a PID design. The design of the high-level controller is not the main contribution of the present work.

3.2 Optimal Control Allocation (OCA)

The OCA calculates the control signals for the low-level controllers using the generalized control input M_{zc}. The allocation of the generalized control signal is accomplished thanks to an optimization process. The optimizer calculates the low-level control signals by minimizing an objective function subject to constraints related to the physical limits of the actuators. Let us emphasize that the design of the high-level controller is independent of the physical vehicle architecture. Different physical vehicle architectures could be handled through an appropriate formulation of the OCA problem.

The OCA layer distributes optimally the global corrective yaw moment on the set of available actuators. Based on (1b), (2), the corrective yaw moment M_{zc} generated by the active stabilization control can be written as follows:

$$M_{zc} = BF \quad (12)$$

$$B = [(a\sin\delta + c\cos\delta)\ \ (a\sin\delta - c\cos\delta)\ \ c\ \ -c] \in \mathbb{R}^{1\times 4} \quad (13)$$

$$F = [F_{l_1}\ \ F_{l_2}\ \ F_{l_3}\ \ F_{l_4}]^T \in \mathbb{R}^4 \quad (14)$$

where B is the effectiveness matrix and F the vector forces.

The OCA problem is then to calculate the longitudinal forces F_{l_i} given by (14) to generate the desired yaw moment by solving the optimization problem:

$$F^* = \arg\min_F \|M_{zc} - BF\| \quad (15)$$

subject to the physical constraints:

(1) $F_{min} \le F \le F_{max}$: the forces are constrained within a certain range.
(2) $\Delta F_{min} \le \Delta F \le \Delta F_{max}$: the force rates are also within a given range.

Remark: constraints on the force rates can be easily handled by rewriting the problem in a discretized form. At a given time instant k the forces vector is $F(k) = F(k-1) + \Delta F$, the problem is then rewritten as follows:

$$\Delta F^* = \arg\min_{\Delta F} \|(M_{zc}(k) - BF(k-1)) - B\Delta F\| \quad (16a)$$

subject to :

$$F_{min} - F(k-1) \le \Delta F \le F_{max} - F(k-1) \quad (16b)$$

$$\Delta F_{min} \le \Delta F \le \Delta F_{max} \quad (16c)$$

The constrained optimization problem (15) can be solved using appropriate numerical algorithms. Among the available optimisation algorithms, an interior point algorithm developed by [Härkegard, 2003] is used here. However, it is hard to give guarantees on the maximum number of iterations and computation time needed to find the optimal solution. Hence, some degree of sub-optimality may need to be accepted in order to fit the real-time limits [Johansen and Fossen, 2013].

3.3 Low-level Controller (LC)

The OCA calculates the longitudinal forces to be generated at the wheels. The low-level controller takes as reference these signals and calculates the physical control input. Here, the physical control inputs are the brake torque for each wheel and the torque differential input. The low-level control for the brakes is an ABS-like system, such as proposed in [Tanelli and A. Astolfi, 2008]. For torque transfer generation several solutions exist, an example of a torque differential is presented in [Hancock et al., 2005].

4. COMPARISON OF CONVENTIONAL DIRECT YAW CONTROL STRATEGIES

In this section, two conventional techniques for DYC are presented and compared. The first one is Brake-based DYC (B-DYC) based on individual braking of each wheel. The second one is Torque Transfer-based DYC (TT-DYC) based on a redistribution of the traction torque.Both strategies are studied to show their merits and limitations. The architecture proposed in Section 3 is adapted at the OCA layer to suit the set of available actuators according to the employed DYC strategy.

4.1 Brake-based Direct Yaw Control (B-DYC)

The differential braking for generating direct yaw moment is widely used in the literature [Shibahata, 2005]. The high-level controller is the same as presented in Section 3 and the control allocation problem is formulated considering individual wheels braking. The OCA calculates the vector of braking forces F_b to generate the desired yaw moment by solving the optimization problem:

$$F_b^* = \arg\min_{F_b} \|M_{zc} - B_b F_b\| \tag{17}$$

where the effectiveness matrix B_b and the desired vector forces F_b respectively given by:

$$B_b = [(a\sin\delta + c\cos\delta) \;\; (a\sin\delta - c\cos\delta) \;\; c \;\; -c] \in \mathbb{R}^{1\times 4} \tag{18}$$
$$F_b = [F_{l_1} \;\; F_{l_2} \;\; F_{l_3} \;\; F_{l_4}]^T \in \mathbb{R}^4$$

subject to the physical constraints:

(1) $F_b \leq 0$: the braking forces are negative.
(2) $F_{b_{max}} \leq F_b$: the maximum braking forces depends on the vertical load and lies within the friction circle (see (7)).
(3) $\Delta F_{b_{min}} \leq \Delta F_b \leq \Delta F_{b_{max}}$: the maximum braking force rate.

A low-level controller then calculates the corresponding braking torque to be applied on the wheel. The design of this controller is out of the scope of this paper (e.g. see [Tanelli and A. Astolfi, 2008] and references therein).

4.2 Torque Transfer based Direct Yaw Control (TT-DYC)

In torque transfer DYC, when a corrective yaw moment should be generated the traction torque is transferred from the outer wheel to the inner one. For the design of the TT-DYC the hierarchical control architecture (cf. Section 3) is also employed. Using a conventional front traction vehicle only the front longitudinal forces are used by the torque differential. These forces are calculated following the same OCA approach, as formulated in (15) by modifying the effectiveness matrix B and the desired vector forces F as follows:

$$B_t = [(a\sin\delta + c\cos\delta) \;\; (a\sin\delta - c\cos\delta)] \in \mathbb{R}^{1\times 2} \tag{19}$$
$$F_t = [F_{t_1} \;\; F_{t_2}]^T \in \mathbb{R}^2$$

and the constraints relative to the torque transfer configuration:

(1) $F_{t_{min}} \leq F_t \leq F_{t_{max}}$: the forces induced by the torque transfer are constrained and lies within the friction circle.
(2) $\Delta F_{t_{min}} \leq \Delta F_t \leq \Delta F_{t_{max}}$: the maximum force rate which depends directly in the maximum rate of torque transfer.
(3) $F_{t_1} = -F_{t_2}$: the torque is transferred from a wheel to another on the same axle, here, it is the front axle.

A torque differential ensures the torque transfer which is needed to generate the required longitudinal forces. Examples of torque differential are described in [He et al., 2006, Hancock et al., 2005].

4.3 Simulation Results

The merits and the limitations of the B-DYC and TT-DYC stabilization strategies are shown through simulation results. The sine with dwell manoeuvre described in Section 2.2 is performed at constant entering speed on a wet test track.

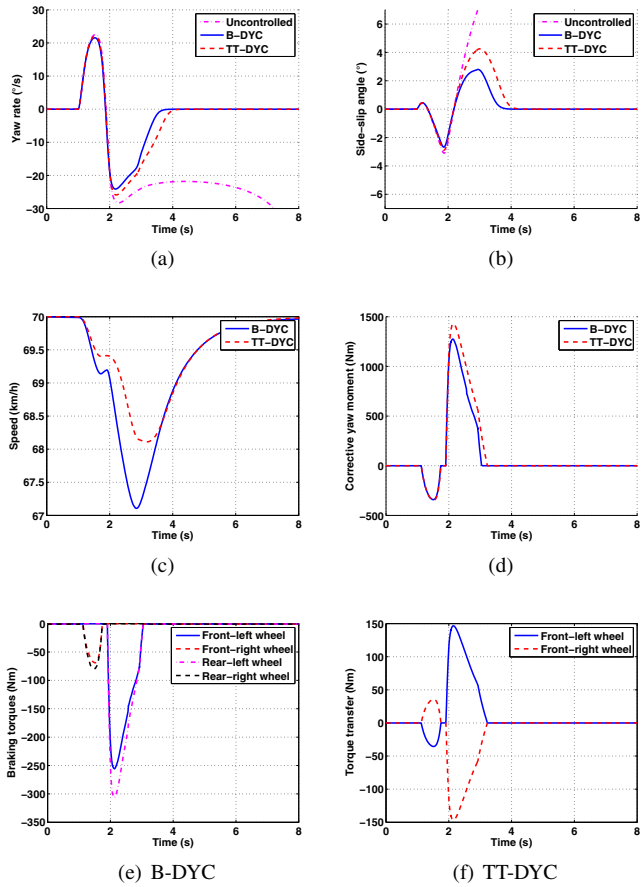

Fig. 4. Brake-based vs. torque transfer direct yaw control

The response of the uncontrolled vehicle as well as the vehicle equipped with a stabilizing controller (B-DYC and TT-DYC) are presented. It can be noticed in Fig. 4 that the equipped vehicle performs safely the manoeuvre while the uncontrolled vehicle losses its stability. The yaw rate and sideslip plots highlight the stabilizing fact of the DYC strategies. The simulation results help also to establish a comparison between the B-DYC

and TT-DYC strategies. It can be observed in Fig. 4(f) the evolution of the vehicle longitudinal speed in both cases. In the case of a B-DYC the vehicle speed is reduced significantly due to brakes action. However, further simulation results showed that stabilization capabilities of the TT-DYC are limited compared to B-DYC. In fact, the same manoeuvre performed at $100\,km/h$ showed that only the B-DYC stabilization is still effective.

4.4 Discussion

It is well known that the brake based DYC is a powerful system for maintaining lateral stability of the vehicle. However, its major drawback is the strong influence on the longitudinal motion limiting its use to only highly extreme driving situations. On the other hand, the torque transfer DYC provides good stabilization capabilities weakly affecting longitudinal motion. However, the stabilization performance is only ensured in a limited operating range. For example, in an under-steer situation, torque is transferred from the outer driving wheel to the inner driving wheel to generate the corrective yaw moment. In this situation, the vertical load on the inner wheel is decreased due to lateral load transfer. In such configuration, excessive torque transfer may cause the inner wheel spinning and consequently the loss of steerability of the vehicle. Therefore, the torque distribution DYC is used in a limited stabilization range and could not replace the brake based DYC [He et al., 2006]. To capitalize the advantages of both stabilizing strategies, i.e. ensure high stabilization capabilities and reduce the impact on the longitudinal motion, the brake based and the torque distribution DYC are integrated in a whole stabilizing strategy.

5. DUAL-MODE CONTROL ALLOCATION FOR INTEGRATED DIRECT YAW CONTROL

The discussion in the previous section showed the benefits of combining in an integrated stabilizing strategy the brake based and the torque transfer DYC. The control strategy proposed here fits in the hierarchical architecture presented in Fig. 3. The high-level control is kept the same and the control allocation problem is reformulated to handle both of stabilizing strategies. The corrective yaw moment is still generated by differential longitudinal forces. However, these forces could be generated differently using brake or torque transfer. Each wheel can be braked conventionally or braked/driven through torque transfer. Note that, the previously presented OCA do not allow to distinguish the different operating modes of the actuators. A dual-mode OCA formulation is proposed here to cope with this limitation.

The dual-mode OCA formulation allows to describe the contribution of each actuator in a given operating mode. The main idea is to introduce a *virtual actuator* for each additional operating mode as proposed in [Chen and Wang, 2012]. Here, for a wheel i two forces F_{b_i} (resulting from brake action) and F_{t_i} (resulting from torque transfer) contribute to generate the whole longitudinal tire force:

$$F_{l_i} = F_{b_i} + F_{t_i} \tag{20}$$

Under these considerations and using (19) and (20), the force vector is given by:

$$F = [F_{b_1}\ F_{b_2}\ F_{b_3}\ F_{b_4}\ F_{t_1}\ F_{t_2}]^T \in \mathbb{R}^6 \tag{21}$$

and the corresponding effectiveness matrix:

$$B = [(a\sin\delta + c\cos\delta)\ (a\sin\delta - c\cos\delta)\ c\ -c\ (a\sin\delta + c\cos\delta)\ (a\sin\delta - c\cos\delta)] \in \mathbb{R}^{1\times 6} \tag{22}$$

The OCA problem is then formulated as follows:

$$F^* = \arg\min_F \|M_{zc} - BF\| \tag{23}$$

subject to the physical constraints:

(1) $F_{b_i} \leq 0$: the braking forces are negative.
(2) $F_{t_{min}} \leq F_t \leq F_{t_{max}}$: the forces due to torque transfer are either positive or negative and constrained by the maximal allowed torque transfer.
(3) $F_{t_1} = -F_{t_2}$: the torque is transferred from a wheel to another on the front axle.
(4) $F_{b_{i=1,2}} + F_t \geq F_{max}$: at the front axle, the total longitudinal forces that can be generated at the tire depends on the vertical load and satisfy the friction circle.
(5) $F_{b_{i=3,4}} \leq F_{max}$: at the rear wheels only the braking forces are considered and satisfy the friction circle.
(6) $\Delta F_{min} \leq \Delta F \leq \Delta F_{max}$: the maximum force rate which depends on the maximum brake and torque transfer rates.
(7) $F_{t_i} F_{b_i} \geq 0$ for $i = 1,2$: the control allocator should ensure exclusivity between brake and traction for the front wheels i.e. solve conflictual situation between brake and torque transfer.

The dual-mode OCA approach is used in order to distinguish the different operating modes of the wheel i.e. conventionally brake and torque transfer. Remark that physically, only the four longitudinal forces corresponding to the four wheels are available. However, the proposed dual-mode formulation employs two additional forces to describe the contribution of the torque transfer on the front axle. The conflicts management between these forces are resolved through the exclusivity constraint (7), the control allocator ensures that a wheel could never be braked and driven at the same time.

This formulation helps also to prioritize the use of torque transfer regarding the brake for stabilization. The secondary objective of the dual-mode OCA consists in minimizing the effects of the stabilization on the longitudinal motion. This is handled through the modification of the cost function by introducing a penalty cost in the optimization problem (23). Finally, the modified objective function is given by:

$$J = \|M_{zc} - BF\| + F^T W F \tag{24}$$

where $W \in \mathbb{R}^{6\times 6}$ is a weighting matrix:

$$W = \gamma \begin{bmatrix} I_{4\times 4} & 0 \\ 0 & 0_{2\times 2} \end{bmatrix} \tag{25}$$

the γ is strictly positive weighting coefficient. Note that only the braking forces induced by conventional braking are penalized. The distinction between the different operating modes for each wheel is made possible thanks to the dual-mode formulation.

5.1 Simulation Results

The integrated stabilization strategy is tested through simulation using the same high-level controller and in the same simulation conditions, i.e. dwell sine manoeuvre on a wet test track. Simulation results given in Fig. 5 show the response of the vehicle equipped with the integrated-DYC. The response of the vehicle equipped with the B-DYC is also presented, for the sake of comparison the same high-level control is used for

the two strategies. Notice, from the yaw rate and sideslip angle plots, that the integrated-DYC strategy shows more stabilization capabilities. In fact, the dwell sine manoeuvre is performed at higher speed ($90\,km/h$) compared to the test presented in Section 4.3. Furthermore, the effects on the longitudinal speed are reduced thanks to the use of torque transfer. Fig. 5(c) shows the evolution of the longitudinal speed in both of cases. Fig. 5(f) shows that both conventional strategies are used in an integrated way following the required stabilization effort. In fact, for the first stabilization action (from $t = 1\,s$ to $t = 2\,s$) only torque transfer is used. For the second stabilization action (from $t = 2\,s$ to $t = 4\,s$) the brakes are also used because the torque transfer is saturated and more stabilization moment is required. This prioritization of the torque transfer is obtained thanks to the dual-mode OCA formulation.

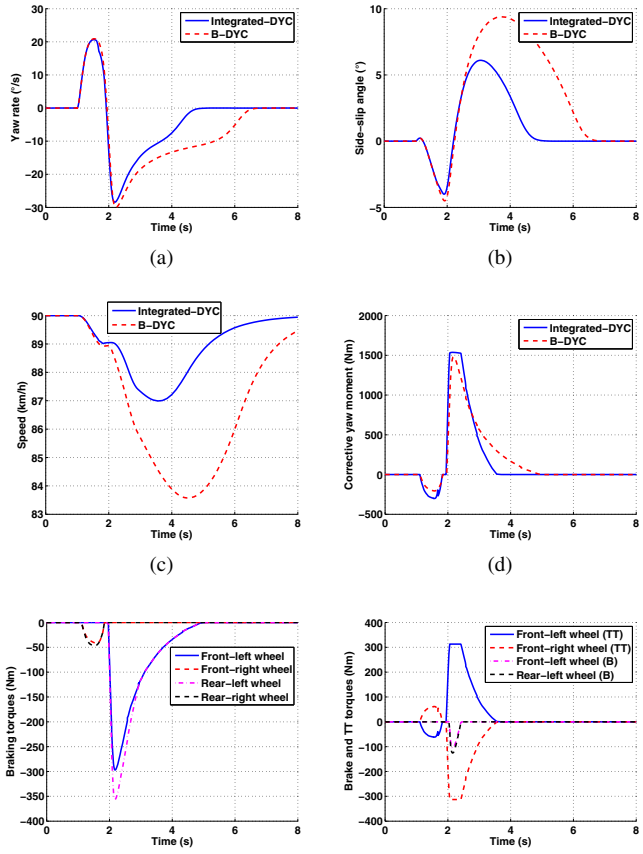

Fig. 5. Proposed integrated-DYC vs. B-DYC

6. CONCLUSIONS

The integrated chassis control by combining brake and torque transfer has been explored in this paper. A hierarchical control architecture has been proposed to meet this objective. The hierarchical structure is composed of high-level and low-level controllers linked through an optimal control allocation layer. The integrated control is based on a dual-mode control allocation formulation combining brake and torque transfer for direct yaw control. The combination of these two systems allows to capitalize the advantages of each one and to overcome the limitations due to the large influence of the brakes on the longitudinal dynamics. Simulation results showed the effectiveness of the proposed control architecture and the advantages brought by the integrated approach. The results showed also the genericity of the proposed control architecture through control allocation formulation. In fact, only the OCA layer is modified to adapt the control strategy to different physical architectures depending on the available actuators.

REFERENCES

M. B. Alberding, J. Tjonnas, and T. A. Johansen. Nonlinear hierarchical control allocation for vehicle yaw stabilization and rollover prevention. In *European Control Conference (ECC'09)*, 2009.

J. Andreasson. *On Generic Road Vehicle Motion Modelling and Control*. PhD thesis, Royal Institute of Technology, Sweden, 2007.

Y. Chen and J. Wang. Fast and global optimal energy-efficient control allocation with applications to over-actuated electric ground vehicles. *IEEE Trans. on Control Systems Technology*, 20:1202–1211, 2012.

G. J. Forkenbrock, D. Elsasser, and B. O'Harra. NHTSA's Light Vehicle Handling and ESC Effectivness Research Program. Technical report, National Highway Traffic Safety Administration, 2005.

M. J. Hancock, R. A. Williams, T. J. Gordon, and M. C. Best. A Comparison of Braking and Differential Control of Road Vehicle Yaw-Sideslip Dynamics. *J. Automobile Engineering*, 219 Part D:309–327, 2005.

J. He, D. A. Crolla, M. C. Levesley, and W. J. Manning. Coordination of active steering, driveline, and braking for integrated vehicle dynamics control. *J. Automobile Engineering*, 220 Part D:1401–1421, 2006.

O. Härkegard. *Backstepping and Control Allocation with Applications to Flight Control*. PhD thesis, Linköping University, Sweden, 2003.

O. Härkegard and S. T. Glad. Resolving actuator redundancy-optimal control vs. control allocation. *Automatica*, 41:137–144, 2005.

T. H. Hwang, K. Park, S. J. Heo, S. H. Lee, and J. C. Lee. Design of integrated chassis control logics for afs and esp. *International Journal of Automotive Technology*, 9 No. 1:17–27, 2008.

T. A. Johansen and T. I. Fossen. Control allocation - A survey. *Automatica*, 49:1087–1103, 2013.

U. Kiencke and C. Nielsen. *Automotive Control Systems*. Springer-Verlag, 2000.

E.K. Liebemann, K. Meder, J. Schuh, and G. Nenninger. Safety and Performance Enhancement: The Bosch Electronic Stability Control (ESP). Technical report, National Highway Traffic Safety Administration (NHTSA), 2004.

Y. Shibahata. Progress and future direction of chassis control technology. *Annual Reviews in Control*, 29:151–158, 2005.

M. Tanelli and S. M. Savaresi A. Astolfi. Robust nonlinear output feedback control for brake by wire control systems. *Automatica*, pages 1078–1087, 2008.

P. Tondel and T. A. Johansen. Control allocation for yaw stabilization in automotive vehicles using multiparametric nonlinear programming. In *American Control Conference*, Portland, USA, 2005.

J. Yoon, W. Cho, J. Kang, B. Koo, and K. Yi. Design and evaluation of a unified chassis control system for rollover prevention and vehicle stability improvment on a virtual test track. *Control Engineering Practice*, 18:585–597, 2010.